Environ Earth Sci (2017) 76:25
DOI 10.1007/s12665-016-6345-3

ORIGINAL ARTICLE

Integration of seismic and sedimentological methods for analysis of Quaternary alluvial depositional systems

Marta Prekopová[1] · Juraj Janočko[1] · Vladimír Budinský[1] · Martina Friedmannová[2]

Received: 29 February 2016 / Accepted: 15 December 2016 / Published online: 24 December 2016

Abstract Due to the high potential of unconsolidated sedimentary bodies to form aquifers and reservoirs, an identification of their exact geometry and location is of great importance. Current conceptual models of these bodies are often developed using scattered data from hydrogeological wells. More reliable results can be achieved by application of methods that can provide continuous subsurface record of the actual geological situation in the investigated area. In this article, a combination of two different approaches is used on a case study of alluvial Quaternary sediments from the East Slovakian Basin, including the discussion how these methods contribute to the final geological interpretation. First, a sedimentological analysis was performed with the use of data acquired from auger drilled hydrogeological wells, which enabled identification of depositional processes, depositional systems and the possible source areas. Due to the shallow depth of the studied area, a second approach based on the geophysical measurement using seismic refraction and tomography was applied. This method provided information mainly about the geometry of these systems, the position of the sediments within them and highlighted where the main changes in the sediment texture and composition occurred. Integration of both methods allows us to obtain a more precise image of the subsurface, which contributes to a better understanding and prediction of the occurring sediments in the studied area.

✉ Marta Prekopová
marta.prekopova@tuke.sk

[1] Institute of Geoscience, Technical University of Košice, Park Komenského 15, 040 01 Kosice, Slovakia

[2] HGM Žilina, Stárkova 26, 010 01 Zilina, Slovakia

Keywords Fluvial · Alluvial · Sedimentology · Quaternary · Seismic refraction · Seismic tomography

Introduction

Recently, there is an increasing interest in studying Quaternary alluvial sediments because of their potential to form aquifers or reservoirs for groundwater and hydrocarbons. In the present work, we put a great emphasis on understanding the spatial distribution of sedimentary bodies. This requires not only a theoretical understanding of alluvial depositional systems, their processes and sediments, but also obtaining their characteristic data from the field.

Since modern alluvial sediments often underlie flat terrain without outcrops, their study usually relies on hydrogeological surveys providing robust but generalized information about the texture of sediment, but these investigations are rarely able to determine their structure.

Data from auger drilling collected in archives and publications usually represent isolated 1D/2D point data sometimes emplaced in the context of cross sections (DeCelles et al. 1991). However, the shallow occurrence of Quaternary sediments predestines their study by application of indirect geophysical methods such as seismic refraction. In spite of the spatially limited data from wells, the seismic refraction can provide continuous 2D sections of the geological situation under the surface.

In this paper, we would like to demonstrate the differences between outcomes resulting from the application of sedimentological and geophysical approach individually and to highlight how their integration can improve the final interpretation of the studied area. Besides this, our aim was to give an overall interpretation of the processes that are active during the deposition of sediments, to identify

depositional systems recorded by preserved sediments and to contribute to the explanation of the geological evolution of the investigated area. Finally, the application of these methods was used to verify the identification of aquifers/aquitards, in which their hydrodynamic function depends on a good definition of boundary conditions and of their degree of heterogeneity as described by Torres-Rondon et al. (2013).

Geological setting

The studied area is situated in the western part of the East Slovakian Neogene Basin in the Košice depression which is located in the Western Carpathians (Fig. 1). The location and especially the depth of the projected wells were planned in order to analyse the whole Quaternary succession from its base to the top (Figs. 1, 2). The Quaternary sediments are underlain by Neogene clays that are typified by their green-greyish colour. These were observed at the base of each well, thus ensuring noticeable stratigraphic and spatial borders of the Quaternary package with the older sediments.

Active tectonic movements together with climate oscillation have a significant impact on the evolution and extent of Quaternary sediments (Harvey et al. 2005; Benvenuti and Martini 2002). Their influence is expressed by the distribution and discharge of streams, the main agents and avenues through which the weathered rock debris are carried from a landscape (Allen 1965). The majority of the Quaternary sediments in the studied area are genetically associated with rivers or smaller creeks depositing sediments, either as fluvial sediments or as sediments of alluvial fans. The transport as well as deposition of the sediments here is related to the large SE-flowing Hornád river and to smaller creeks as SE-oriented Črmeľ creek, or to the W-flowing unnamed creek (Fig. 1). The consequence of the uplift trend, which began already at the end of the Neogene along NW–SE, NE–SW and N–S trending faults in the region (Fig. 1), was a sharply modelled relief of the pre-Tertiary units enabling source material to be disposal for further transport.

The oldest Quaternary sediments connected with the cyclic aggradational and erosive activity of the Hornád river are sandy gravels of Pleistocene terraces (Fig. 1). Easily recognizable is the coarsest fraction with size of the particles to 15 cm, considered to represent fluvial lag deposits (Kaličiak et al. 1991). The maturity of the clasts, demonstrated by their subrounded, occasionally rounded shape, suggests their longer transport from the source areas. The variable composition of clasts indicates their different origin, but in general quartz, quartzite, metamorphic rocks, granite, conglomerate, sandstone and carbonates were identified (Kaličiak et al. 1996a, b). Sandy gravels are capped with 2-m-thick clays and sands with marked limonite content thus demonstrating a shift in sedimentation from active fluvial channels to more distal overbank areas (Kaličiak et al. 1996a, b).

During the Upper Pleistocene, a small SE-oriented alluvial fan with radius around 1 km developed (Fig. 1) at the flank of the Spis-Gemer Mts. The composition of the sandy and clayey gravels resembles to the composition of the gravels transported by Hornád river. However, quartz, quartzite, metamorphic rocks as well as conglomerates and carbonate debris are mainly angular to subangular in shape with a weakly sorted and more clayey matrix (Polák et al. 1997).

The activity of rivers and smaller creeks continued also during the Holocene via the deposition of fluvial loams, sands and clays and via formation of small alluvial fans consisting of mainly loamy gravels (Fig. 1).

Methods

Seven shallow hydrogeological wells were drilled across the area of the Technical University in Košice to provide detailed lithological description and groundwater information (Fig. 1). The wells were drilled to a depth of 14 m and were terminated in the greenish-grey Neogene clays. The stratigraphic boundary between Quaternary and Neogene sediments lies usually at the depth between 11 and 13 m; however, in the well 3, this boundary is located deeper at 13.3 m under the surface. Sediments were studied from two different approaches—sedimentological and geophysical.

In order to deduce the depositional processes and environment, a sedimentological analysis was carried out, beginning with a macroscopic assessment of the main characteristics of the sediments (particle size, shape and composition, Wentworth 1922; Powers 1953; Tucker 2003; Boggs 2009). Due to devastating effect of the auger drilling on the sediments structures, the sediment structure seemed and was described as massive and the focus of the analysis turned to the texture of sediments. A total of 12 facies were recognized (Fig. 2) in this analysis. The overall dominance of the gravels in the wells corresponds with the higher amount of gravelly facies (9) which were further differentiated based on their clasts composition and level of roundness (Powers 1953; Boggs 2009).

Grain size analysis of the matrix of 20 gravelly samples (400 g each, Table 1) was based on mechanical sieving with meshes corresponding to the standard Wentworth (1922) grain size classification. Cumulative frequency curves (Fig. 3) were used for calculating statistical parameters including the graphic mean, degree of sorting, asymmetry and kurtosis (Table 1) of the sediments using the formulae of Folk and Ward (1957). The overall shape

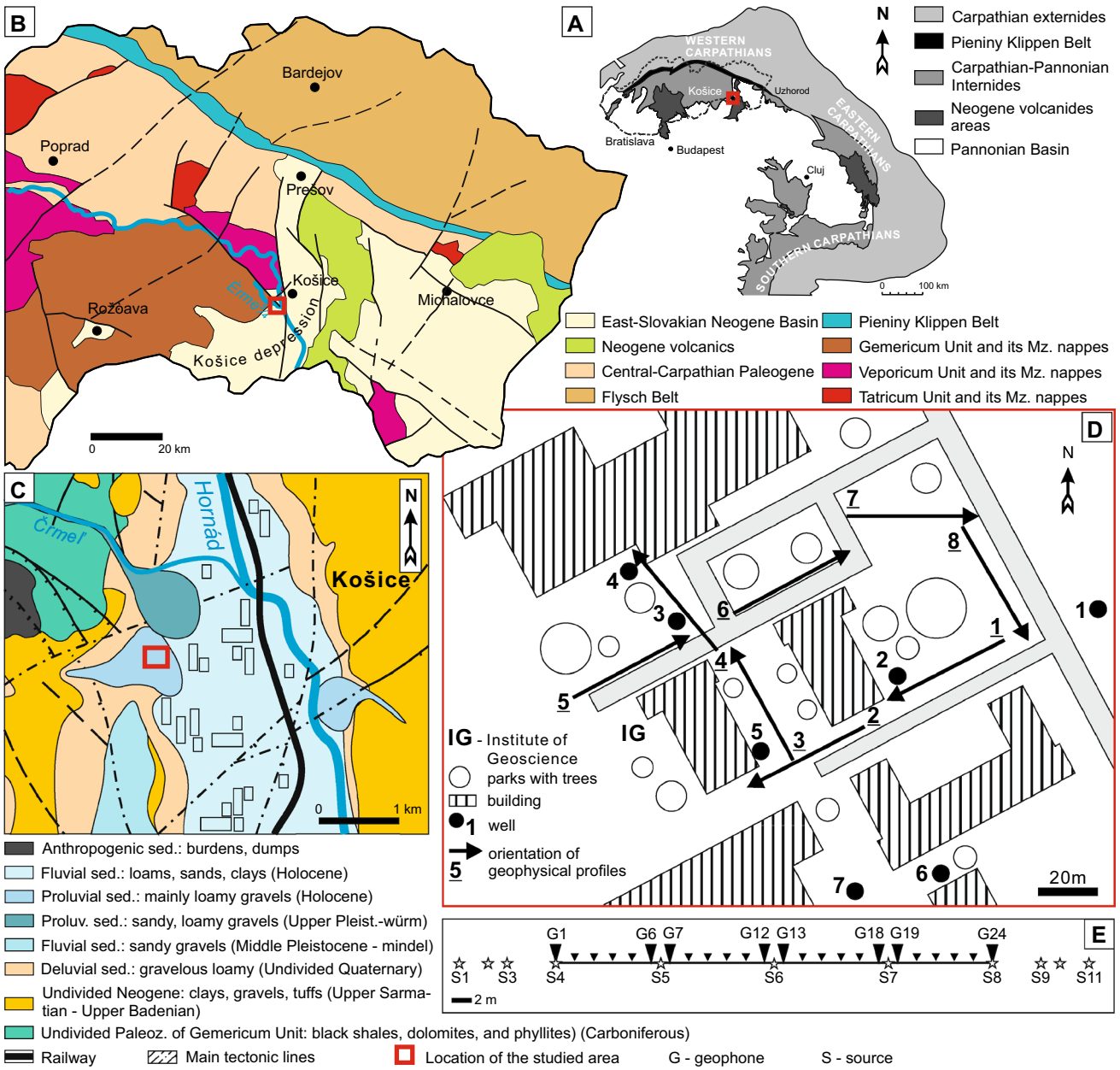

Fig. 1 Studied area forms a part of the East Slovakian Neogene Basin (**b**, modified after Lexa et al. 2000) in the internides of the Western Carpathians (**a**, modified after Kováč et al. 1998). Fluvial sediments as well as sediments of alluvial fans prevail in the area of Technical University of Košice (**c**, modified after Kaličiak et al. 1996a, b, Polák et al. 1996). Seven hydrogeological wells were drilled, and eight geophysical profiles were measured in the area (**d**). The setting of the 46-m-long profiles (**e**): geophone offset = 2 m, sampling interval 100 μs, number of samples = 2048, record time = 204.8 ms and number of stacks = 2

of the curves refers not only to the grain size distribution of the matrix, but it can indicate the aspects of flow regime and depositional environment (Skaberne 1996; Remaitre et al. 2005; Cheetham et al. 2008; Amireh 2015).

The second approach was based on application of seismic refraction. Eight seismic profiles were located in the vicinity of the drilled wells (Fig. 1). The field data were collected using 10-Hz geophones and a Terraloc Mk8 seismograph. The geophone offset was 2 m, thus achieving 26-m-long profiles. A 5-kg hammer created energy by impacting a steel plate at the ground surface. Two stacks were recorded at each shot point. The shots were located at the distance 10, 7 and 5 m from the first and the last geophones, also near the G1 and G24 and between G6–G7, G12–G13 and G18–G19. The measurement array as well as the basic setting of the seismograph is displayed in Fig. 1.

Data from the seismic survey were processed using ReflexW Sandmeier scientific software Version 7.2.2 and

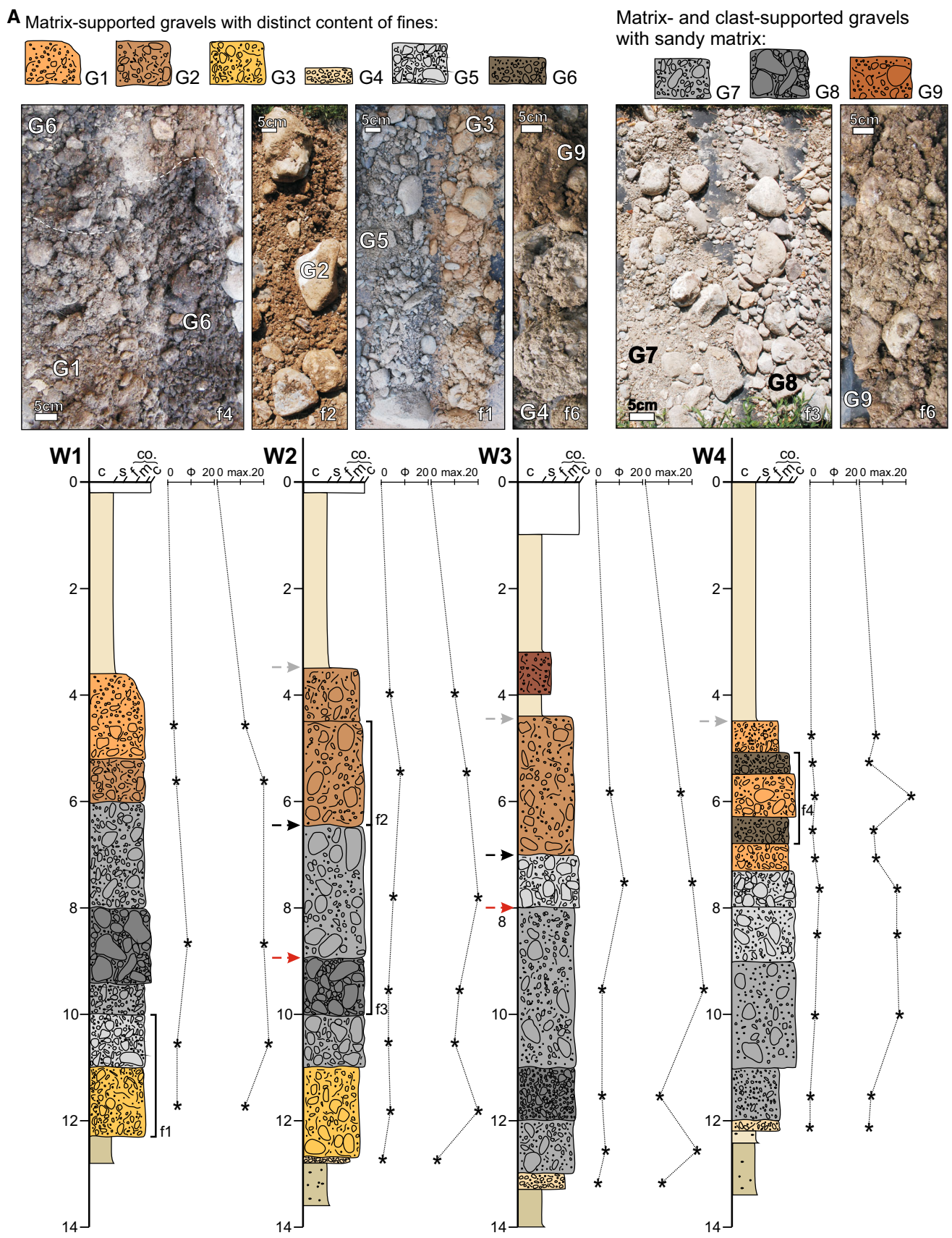

◀**Fig. 2** Together, 12 facies were recognized within the succession: m-s gravels with distinct content of fines (G1–G6), m-s and c-s gravels with sandy matrix (G7–G9), sandy facies (S1) and fine-grained homogeneous deposits (F1 and F2). The refraction line (*red arrow*) marks the border between m-s and c-s facies (G7 and G8, W2), m-s facies with different content of fines and grain size (G5 and G7, W3) or it lies at the contact of fines with c-s gravels (F1 and G8, W5). Borders between velocity "packages" recognized by tomography are marked by *grey* (first and second) and *black* (second and third) arrow, respectively

started with manual selection of the first-arrival information from the raw data followed by a travel-time analysis (Fig. 4). The combined travel times were the basis for a subsequent 2D wavefront inversion which resulted in formation of the preliminary 2D velocity–depth models with two refraction boundaries.

To start the tomographic inversion, an initial start model was needed. Here, we used a simple 1D homogeneous model with a velocity of 500 m/s at the surface boundary. For the resultant model, data saved from the manually picked files were loaded, a space increment of 0.7 was chosen and 20 iterations were processed (profile 1). The curved rays were calculated using a finite difference approximation of the Eikonal equation. Finally, the tomographic result was controlled via checking the mean travel-time difference between the calculated travel times (from tomographic model) and the observed travel-time data. Despite of the visualization of the tomographic models with the refraction boundaries within the same profiles (Figs. 4, 5), it is important to emphasize that they represent individual outcomes. After overlapping and comparison of the resultant tomographic profiles with wells, a good correlation between sediment and velocity distribution was observed and led us to identification of three velocity packages (Figs. 4, 5).

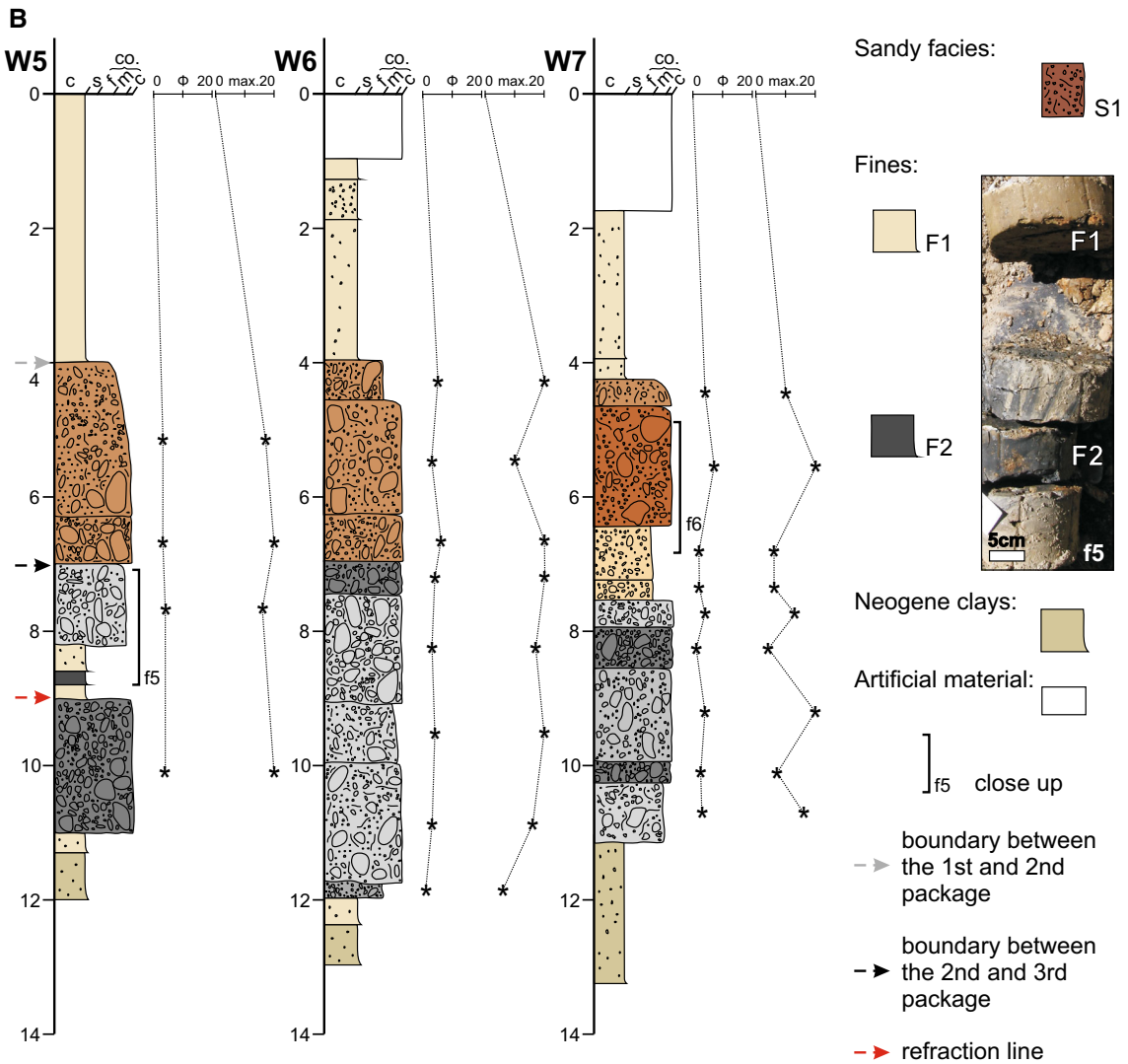

Fig. 2 continued

Table 1 Basic statistical analysis of the matrix after mechanical sieving

	Facies	Well	Depth (m)	Mean (cm)	Class	Bed thickness (m)	Graphic mean (Φ)	Matrix	Fines (%)	Sorting		Asymmetry		Kurtosis	
1	G1	1	4.5	3	Pebbly gravel	1.6	1.07	Medium sand	16.25	2.65	Very weak	0.2	Fine skewed	0.95	Mesokurtic
2	G1	4	7.1	2	Pebbly gravel	0.3	0.5	Coarse sand	14.33	2.84	Very weak	0.51	SS towards fines	1.35	Leptokurtic
3	G2	2	5.3	8	Cobbly gravel	2	0.97	Coarse sand	18	2.96	Very weak	0.44	SS towards fines	1.06	Mesokurtic
4	G2	3	5.8	4	Pebbly gravel	2.6	–0.03	VC sand	11.5	2.23	Very weak	0.25	Fine skewed	1.48	Leptokurtic
5	G5	3	7.8	12	Cobbly gravel	1	1.27	Medium sand	20.75	2.87	Very weak	0.38	SS towards fines	0.91	Mesokurtic
6	G5	4	8.1	4	Cobbly gravel	1	0.63	Coarse sand	15.75	2.91	Very weak	0.44	SS towards fines	1.06	Mesokurtic
7	G5	6	8.1	3	Pebbly gravel	1.5	0.23	Coarse sand	8.25	2.26	Very weak	0.31	SS towards fines	1.14	Leptokurtic
8	G5	5	7.7	4	Pebbly gravel	1.2	0.3	Coarse sand	6.25	2.23	Very weak	0.14	Fine skewed	1	Mesokurtic
9	G6	4	6.7	1	Pebbly gravel	0.4	–0.73	VC sand	11.25	2.17	Very weak	0.37	SS towards fines	1.56	Very leptokurtic
10	G9	7	5.3	7	Cobbly gravel	1.3	–0.43	VC sand	0.75	1.61	Weak	0.35	SS towards fines	0.68	Platykurtic
11	G7	1	7.9	–	–	2	–0.67	VC sand	1.25	1.64	Weak	0.0	Symmetrical	0.63	Very platykurtic
12	G7	2	10.2	3	Pebbly gravel	1	–0.33	VC sand	3.25	1.89	Weak	0.1	Symmetrical	1.3	Leptokurtic
13	G7	3	10.6	3	Pebbly gravel	3	–0.33	VC sand	1.75	1.45	Weak	–0.05	Symmetrical	1.21	Leptokurtic
14	G7	3	12.2	4	Pebbly gravel	1	–0.17	VC sand	3.75	1.95	Weak	0.16	Fine skewed	1.09	Mesokurtic
15	G7	4	10.1	2	Pebbly gravel	2	–0.37	VC sand	1.25	1.53	weak	0.06	symmetrical	0.98	Mesokurtic
16	G7	4	11.8	0.7	Pebbly gravel	1	–0.17	VC sand	1	1.67	weak	0	symmetrical	0.8	Platykurtic
17	G7	7	8.9	4	Pebbly gravel	1.4	–0.77	VC sand	1.25	1.7	weak	0.58	SS towards fines	0.91	Mesokurtic
18	G8	3	11.3	3	Pebbly gravel	1	–1.5	gravel	1.41	1.71	weak	0.05	symmetrical	1.06	Mesokurtic
19	G8	5	9.1	4	Pebbly gravel	2	–1.1	gravel	0.77	1.57	weak	0.24	fine skewed	0.95	Mesokurtic
20	Hornád	P1	0.9	1	Pebbly gravel	0.72	–0.07	VC sand	3.67	1.66	weak	0.31	coarse skewed	0.76	Platykurtic

Two groups of facies are differentiated by black line. Matrix of the first nine samples contains more fines (clay and silt together) and displays very weak sorting. Matrix of the samples below the black line contains <3.75% of fines and its sorting is weak. Comparison of the last sample from the fluvial sediments of Hornád river reveals common features with the gravels below the black line (*VC* very coarse, *SS* strongly skewed)

At the end, the results of the both methods were analysed and combined for the final interpretation (Fig. 6).

Sedimentological analysis

Detailed sedimentological observations within the field work led us to recognize 12 different facies (Fig. 2). They are gathered into four main groups, from which the coarsest are gravelly sediments which are comprised of 9 facies (G1–G9) divided into (1) matrix-supported gravels with a matrix containing higher amount of fines (silt and mud together) and (2) matrix- to clast-supported gravels with a sandier matrix (Table 1). As a third group, sandy sediments with only one facies (S1) were recognized. The fourth and finally the finest group of sediments consist of fine-grained homogenous deposits with two facies (F1 and F2).

Matrix-supported (m-s) gravels with distinct content of fines (G1–G6)

These are mostly thick-bedded gravelly sediments which are massive and are poorly sorted. Only a few beds tend to show better internal organization and normal grading. The

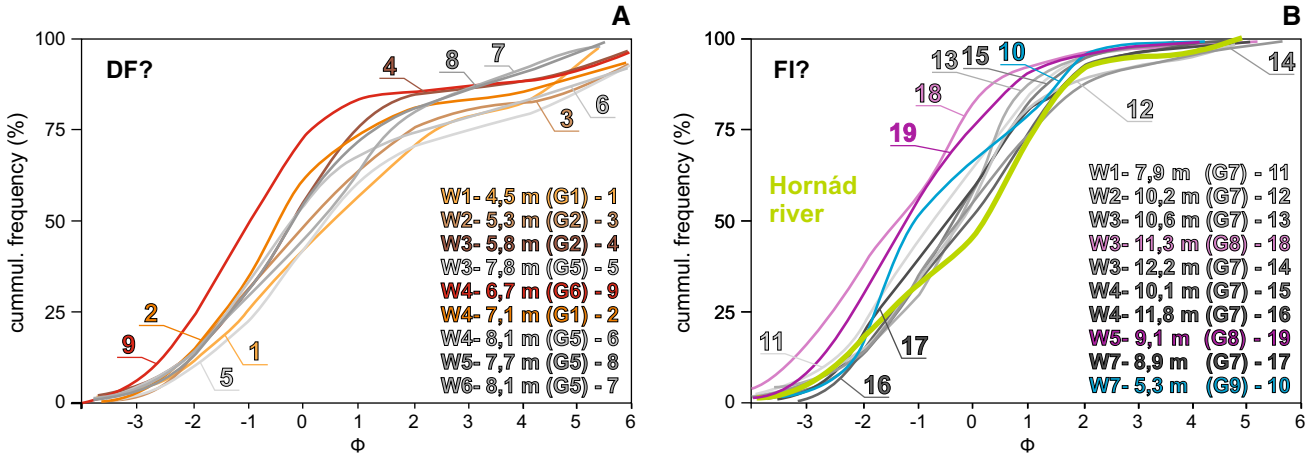

Fig. 3 Two trends of grain size distribution were recognized (**a**, **b**). These correspond with the groups differentiated on the basis of the matrix in Table 1; **a** m-s gravels with distinct content of fines and **b** m-s and c-s gravels with sandy matrix. Grain size characteristics of the sediments indicate their deposition from debris flows (**a**) and from fluidal flows (**b**), respectively (Serra 1985; Wagreich and Strauss 2005). Note the grain size distribution curve of fluvial sediments from the Hornád river (*green*), copying the trend of the curves having fluidal origin

mean size of the fine- to coarse-grained gravels ranges from pebbles to cobbles, but the maximum clast sizes are cobbles or even boulders (more than 20 cm in diameter). Large clasts are floating randomly, but some are settled in vertical position. The matrix is medium- to very coarse-grained sand with granules and a higher content of fines (more than 6.25%). Bed boundaries are usually indistinct, commonly amalgamated, with the thickness of beds reaching up to 2.8 m (W3, Fig. 2).

According to the composition and the degree of roundness of the gravels, most of the facies (5) consist of Palaeozoic metamorphic, magmatic and quartz clasts, which have a subangular to subrounded shape. Differences between the facies are, moreover, highlighted by their colours which we used for their recognition as: *rusty m-s gravel (G1), brown m-s gravel (G2), orangebrown m-s gravel (G3), lightbrown m-s gravel (G4) and darkbrown m-s gravel (G6)*. The only one facies with higher content of carbonate clasts with subangular to subrounded shape is the *greybrown m-s gravel (G5)* (Fig. 2).

The deposition of the massive, unsorted matrix-supported gravel may be related with some form of mass-flow processes. The general characteristics of this facies, such as massive and mostly ungraded nature, chaotic fabric, weak sorting as well as high content of fines, are suggestive of their emplacement by debris flows (Johnson 1970; Kumar et al. 2007). The muddy matrix may indicate "plug" flow deposition of cohesive debris flow (Nemec and Steel 1984; Kumar et al. 2007), in which the en masse deposition proceeds by cohesive freezing (Lowe 1982) as the driving shear stress drops below the yield strength of the viscoplastic substance (Johnson 1984). The massive freezing is also inferred by the poorly sorted matrix supporting the gravels. Crude normal grading visible in a few beds suggests these materials have been deposited from surging flows (Nemec and Steel 1984). Alternatively, these sediments may originate also from hyperconcentrated flows, which represent non-Newtonian turbulent flows operating between normal stream flow and debris flow (Pierson 1970; Pierson and Costa 1987; Nemec 2009). In these flows, the higher content of fines, together with surrounding water, supports the transport of the coarser solid particles of sand and gravel size in suspension (intermittently suspended load) (Pierson 1970). However, the amount of fines does not guarantee that the yield strength was sufficiently high to exhibit plastic flow behaviour and fully suspended gravels in the flow as in the case of debris flows (Pierson and Costa 1987). Pierson (1970) connected the origin of similar deposits with deposition via a very rapid, chaotic suspension fall-out from the deepest and fastest part of the flow where the concentration of sediments is the highest.

The disorganized clast fabric may indicate that the sediments were only transported a short distance, but often suggests non-sheared (high strength) "plug" flow, or only weakly sheared (high-viscosity) flow (Nemec and Steel 1984). Short transport distance can be confirmed by lower level of grounding typical for majority of facies. According to the clast composition, the source area of the most gravel could be represented by nearby subcrops of the Gemericum Unit. However, the higher content of carbonates in the greybrown m-s gravel (G5) could possibly indicate different source area for this facies.

The few metre thick beds can be explained by a series of surges stacked one upon another; thus, their overall thickness do not relate with the thickness of the depositing flow (Sohn 1997). Incremental aggradation of individual

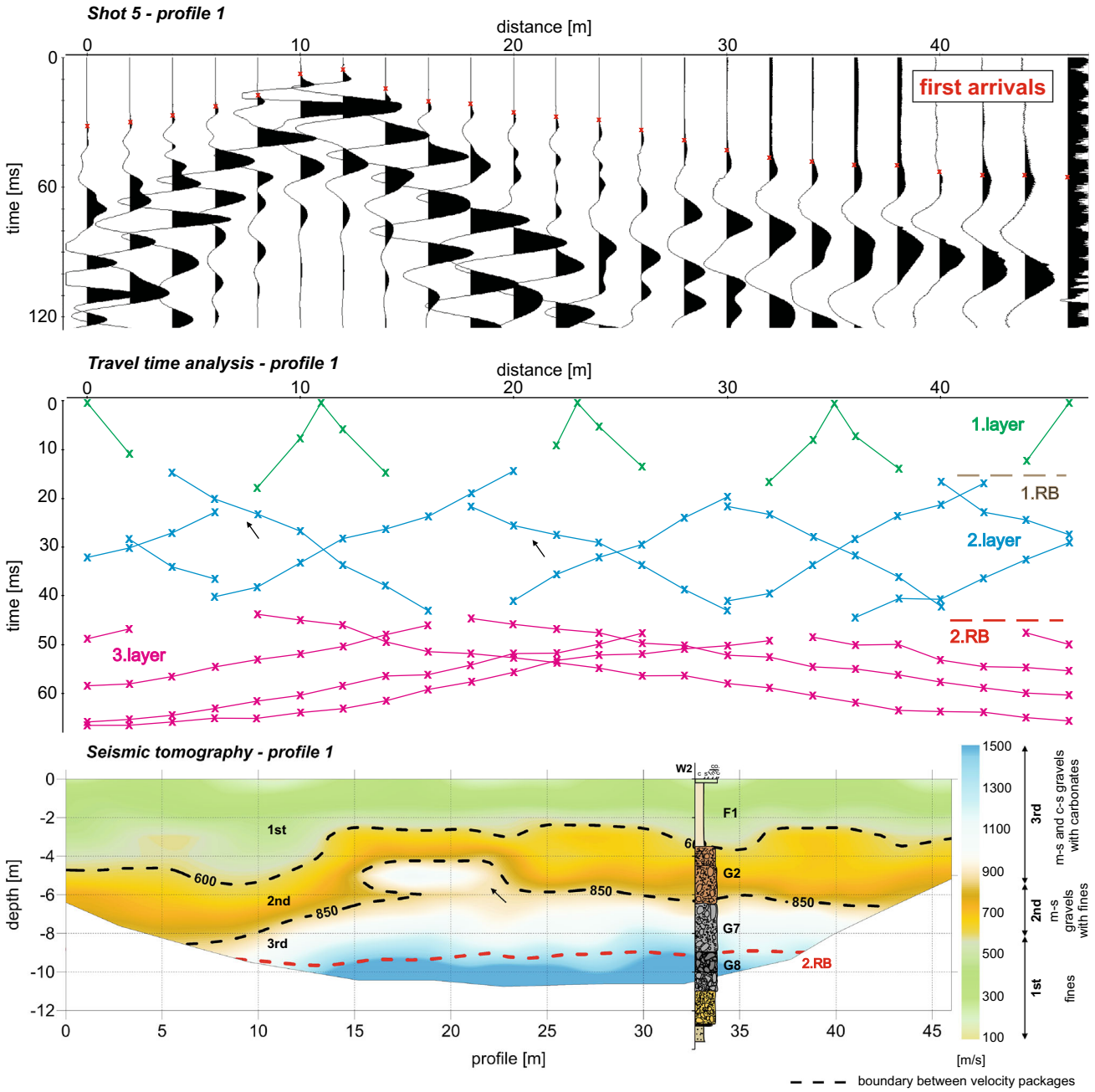

Fig. 4 Processing steps—manual picking of the first arrivals (*red crosses*) and travel-time analysis with three-layer model and two refraction boundaries (1.RB and 2.RB). Note the inversion of the velocities within the second layer which is demonstrated in tomographic profile as a distinct irregularity (marked by *black arrow*). Three "packages" characterized by different seismic velocities were identified in tomographic profiles: fines (first), m-s gravels with fines (second) and m-s and c-s gravels with carbonates (third). The refraction line (*red dashed line*) is passing through the contact between G7 and G8. The facies codes are the same as in the Fig. 2

flows possibly commenced before the consolidation of earlier deposits, resulting in amalgamation of beds (Major 1997; Sohn 1997).

The grain size distribution curves of the facies (Fig. 3a) reveal the dominance of the sandy component in the matrix—the sand content varies between 40 and 62% with an average of 54%. The matrix typically contains a significant amount of fines (to 21%) relatively to the high content of gravels (to 49%). Sorting of the sediment is very weak (Fig. 3a; Table 1). A similar grain size characteristic indicates deposition of sediment by a process that is intermediate between mudflow and water-laid processes (Serra 1985; Lavigne and Thouret 2002; Wagreich and Strauss 2005).

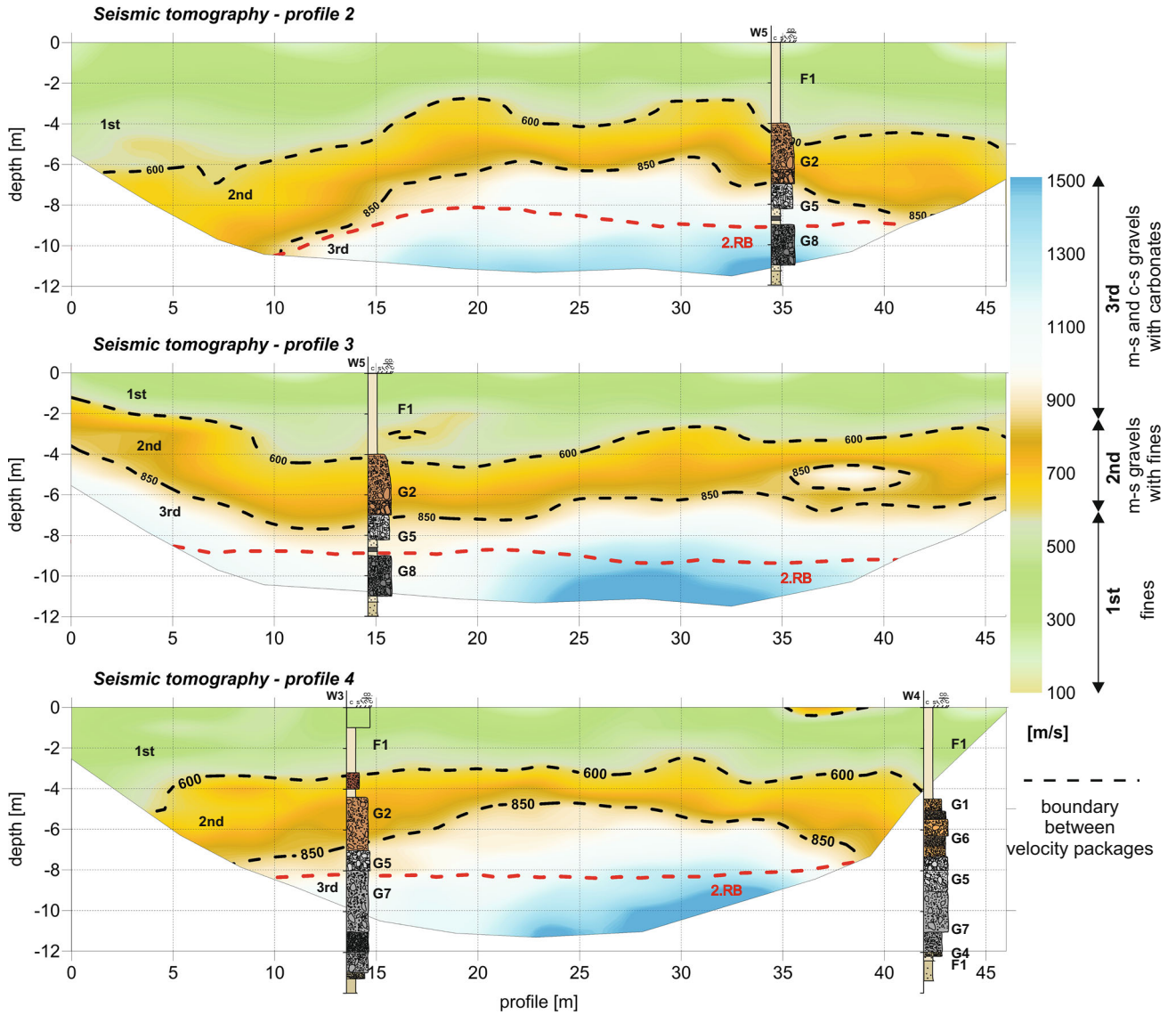

Fig. 5 Tomographic profiles overlapped by refraction boundary and wells. The refraction boundary passes either between fines and G8 (c-s gravels; profile 2 and 3), or between facies G5 and G7 (m-s gravels both, profile 4). Recognition of velocity "packages" (first, second and third) depicts the geometry of the facies which they represent. Seismic tomography was also able to identify 1.5-m-thick and 5-m-long lens (profile 3)

Matrix- and clast-supported (c-s) gravels with sandy matrix (G7–G9)

Beds of matrix- or clast-supported gravels with a sandy matrix can be found in all of the wells (Fig. 2). The medium- to coarse-grained gravels are massive and ungraded. By contrast to the gravels that have been previously described, here the matrix is weakly sorted, very coarse grained sand or gravel with a lesser amount of fines (<3.75%). The diameter of randomly oriented pebbles and cobbles is usually around 10 cm, but outsized boulders with a diameter of up to 30 cm are common as well.

According to their composition and shape, we recognized three facies in this group: *grey m-s gravel (G7)* containing subrounded to rounded, sometimes subangular mainly quartz and carbonate clasts. Very similar in composition and level of roundness is *grey c-s gravel (G8)* differing from the G7 only in the clast-support structure. The *redbrown m-s gravel (G9)* is characterized by prevailing subangular to subrounded clasts of Palaeozoic metamorphics and magmatics. The boundaries between different facies are distinct, but due to the amalgamation of beds, the boundaries within the same facies are difficult to recognize. Therefore, the final thicknesses of beds may reach up to 3 m (W3, Fig. 2).

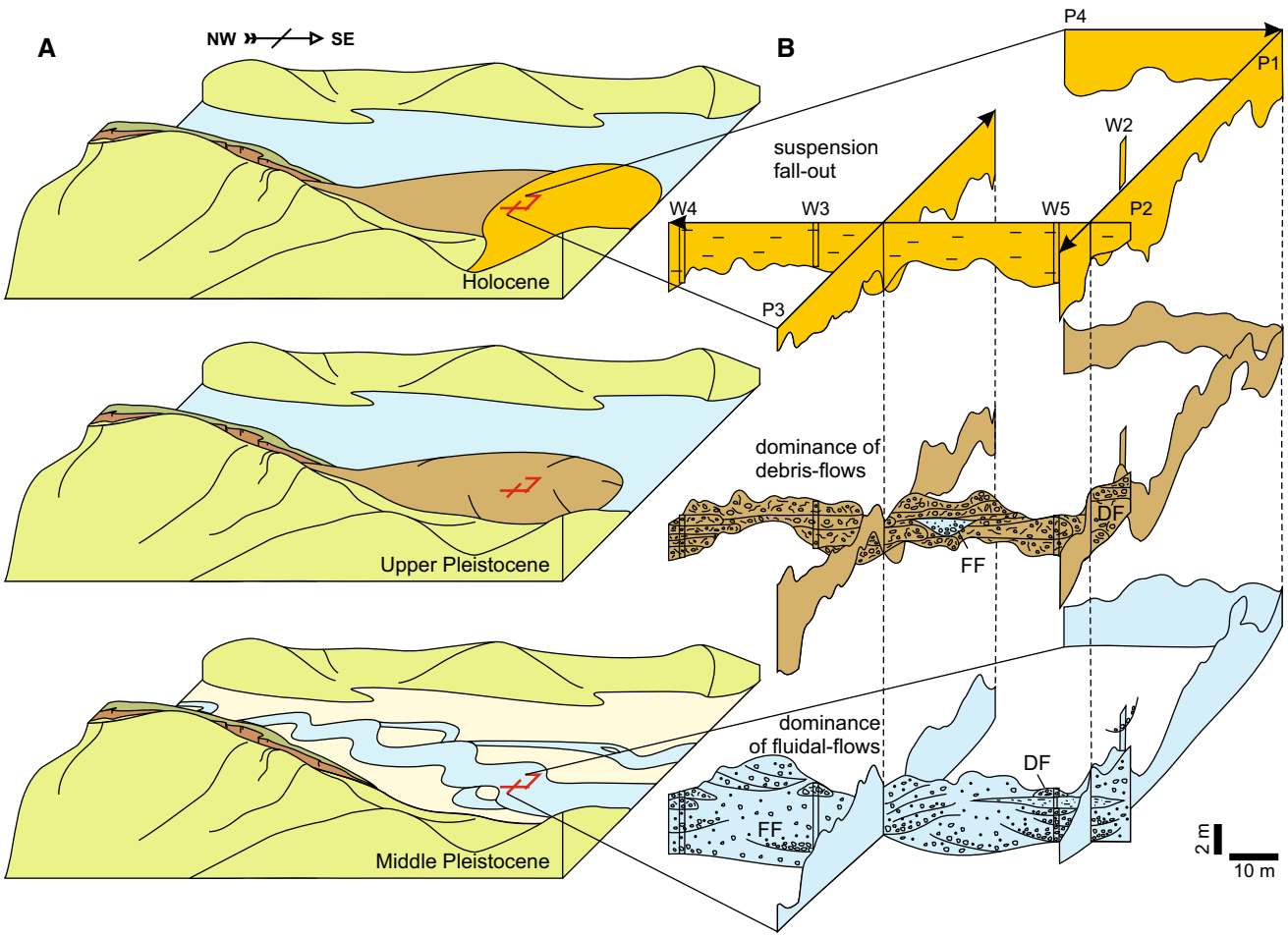

Fig. 6 Evolution of the studied area in time according to sedimentological approach (6**a**): Fluvial activity during Middle Pleistocene was occasionally interrupted by incursions of debris flows. Successive inflows of debris flows during Upper Pleistocene resulted in SE trending alluvial fan. This was during Holocene overlaid by fines of a new alluvial fan headed to the E. Geophysical approach (6**b**) highlighted the geometry of distinct depositional processes and systems (P1 = profile 1 and 2; P2 = profile 3 and 4; P3 = profile 5 and 6, P4 = profile 8; *DF* debris flow, *FF* fluidal flow)

As a consequence of incomplete structural data, the genesis of facies can be interpreted in several ways. First of all, these sediments may be deposited by cohesionless debris flows dominated by frictional grain interactions (Kim et al. 1995; Sohn et al. 1999). The lack of inverse grading and imbrication of clasts could have been caused by the suppression of clast collision (Sohn 1997). Kumar et al. (2007) and DeCelles et al. (1991) connected the origin of similar deposits to rapid deposition from hyperconcentrated flows. An alternative interpretation is that these sediments were deposited from fluidal flow carrying high-sediment bed load and suspended load.

Although the clast-supported nature of the sediments is typical for stream flow, debris flow can also result in this type of structure (Nemec and Steel 1984). However, the subrounded shape of cobbles suggests a long transport distance with effective reworking of clasts. Gravels were probably transported as bed load during the highest stream discharges. Clast-supported pebbles to boulders probably represent lag deposits (Yagishita 1997; Komatsubara 2004) deposited in the deepest part of the channels. Their concentration is highlighted by winnowing of finer materials as sand from initial deposits (Allen 1965). Matrix-supported gravels (sand with scattered pebbles and cobbles) were probably deposited as bars.

The fluidal nature of the flow is also suggested by grain size distribution curves (Fig. 3b). The content of the sand in the matrix is similar to the former group of facies (Fig. 3a). The sand can form 42 to 69% of the matrix or an average of 56%. The main difference is the remarkable lower content of fines (<4%) and slightly higher content of gravels (to 57%) in the matrix (Fig. 3b; Table 1). Better sorting as well as the overall trend of the curves resembles the water-laid deposits of Serra (1985), Skaberne (1996) and Wagreich and Strauss (2005) or stream flow deposits of Lavigne and Thouret (2002). Moreover, the comparison of

the studied grain size distribution curves with the curve of Holocene sediments deposited by the Hornád river in few km distance from the studied locality supports the fluidal origin of these facies (Fig. 3b).

The composition of the clasts as well as their reworking grade indicates several different source areas for the individual facies. Facies G7 and G8 with higher level of roundness were probably transported from the same source area located more distally than the gravels of G9. However, due to the changeable course of the Hornád river crossing several different geological units such as the Veporicum and Gemericum Units or the area of the Central-Carpathian Palaeogene Basin, the more precise identification of their provenance is ambiguous.

Sandy facies (S1)

In the whole area, only one 0.8-m-thick sandy lens intercalated between fines was found (W3, Fig. 2). Angular to subangular, sometimes also subrounded mostly granule, rarely pebble clasts are chaotically dispersed throughout the darkbrown *clayey sand (S1).* Palaeozoic metamorphic rocks dominate in their composition; however, quartz, sandstones and carbonates are also present.

Sand can be moved over a wide range in stages, but less rapidly than the suspended load (Allen 1965). The discontinuous gravelly sandstone bed sandwiched between fines probably represents small recurrent incursions of flows having higher competence as the flow deposited the surrounding fines.

Fine-grained homogeneous deposits (F1 and F2)

Clayey to muddy sediments occur as decimetre-thick discontinuous inter-beds or they form more than 4-m-thick laterally persistent beds in the upper part of the wells. Two types of homogenous deposits were recognized—*brown fines (F1) and dark grey fines (F2).* In general, the facies are devoid of gravel clasts, but sometimes granules and fine pebbles of subangular to subrounded shape are scattered throughout the beds.

Massive fines imply low-energy environment dominated by slow suspension fall-out (Sohn et al. 1999). A long-continued accumulation of fines is associated with floodwaters that became stilled after reaching low-lying depressions (Allen 1965). Fluctuations in the flow strength were inferred from locally accumulated clasts. It manifests the interruption of the low-energy conditions by stronger surges during the flood.

Several processes were responsible for the formation of the sedimentary section. The obvious dominance of gravels suggests conditions, during which flows with high competence able to carry coarser-grains as debris flows, hyperconcentrated flows or stream flows prevail. Auger drilling allowed us to investigate the different transport processes as well as the location and the composition of the source area only from the sediment texture. According to the sedimentological analysis, the origin of the studied deposits is related with four depositional systems. Their alternating activity is recorded by inter-fingering facies of fluvial and alluvial fan systems.

Sedimentation of the Quaternary succession started with short period of debris flows/hyperconcentrated flows incursions, catching sediments from close-lying hills of the Gemericum Unit and depositing them as a part of the alluvial fan.

Successive changes in the environmental conditions during the Middle Pleistocene facilitated the increasing activity of the Hornád river, resulting mainly in more diluted stream flows depositing sediments either as lag deposits in the deepest parts of the channel or as fluvial bars (Fig. 6a). Probably, the low stability of the river banks triggered few incursions of debris/hyperconcentrated flows. Bank collapses are typical for the beginning and the end of the fluvial period. They can be connected with steep and poorly strengthen channel margins. Lenses of fines within the fluvial section probably represent small rarely flooded depressions located laterally and distally from the active fluvial channel.

During the Upper Pleistocene, the fluvial system was replaced by recurrent invasions of debris flows/hyperconcentrated flows from the close Čermeľ valley (Gemericum Unit), thus forming small alluvial fan (Fig. 6a). The overall thickness of the coarse-grained sediments of this section refers to the aggradations of several successive flows. The coarse-grained nature of sediments indicates the proximity of the source area and their deposition area perhaps in a mid-fan lobe (Heward 1978).

The vertical section ends with a 4-m-thick sequence of homogenous fines which were ascribed to Holocene alluvial fan fed from an unnamed creek (Fig. 6a). These sediments were deposited in the quiet condition from slow suspension fall-out either in the inactive segment or in the most distal part of the alluvial fan. The thick accumulations confirm a long period of fan abandonment. The inundated area was occasionally intruded by sheet floods with higher competence, resulting in deposition of thin lenses of gravelly sands. Alternatively, the thickness of the sediments may indicate deposition from more than one system, and then, the sediments can represent overbank facies of fluvial origin.

Changes in clast composition and matrix type between the both Pleistocene sequences were most likely produced by exposure of different source rocks (Sohn et al. 1999). According to Blair and McPherson (2009) and, Harvey et al. (2005), the catchment characteristics, such as its geology, control the primary processes activity of the fan. We conclude that the dominance of cohesion debris flows/

hyperconcentrated flows in the studied alluvial fan section can relate with weathering of pelitic metamorphic rocks of Gemericum Unit during suitable climatic conditions, thus providing abundance fines needed for maintaining the coarser particles in the suspension. By contrast, the presence of granite clasts in the sediments deposited by Hornád river corresponds with the sandier matrix of the fluvial gravels. As stated by Blair and McPherson (2009), the sandier matrix can be produced from granites or gneisses related to physical disaggregation of crystals.

Seismic refraction and seismic tomography

Eight seismic profiles were measured of which five were located close to the wells (Fig. 1). Their locations were planned in order to form a net of cross sections, providing a 3D view of the overall geology of the studied area. The processing of the seismic refraction data led to the identification of two refraction layers. The first layer lying within a 4-m-deep zone probably represents a contact of an artificial material (bricks) often found in the shallow subsurface zone with the clays. This layer was not considered in the analysis; hence, it is not displayed in the profiles.

The second refraction line (red dashed line) can be seen at a depth of 8–9 m under the surface. It passes through the boundary between facies G7 (m-s gravels) and G8 (c-s gravels; profile 1, Fig. 4), G5 (m-s gravel) and G7 (profile 4, Fig. 5) or it marks the contact between F1 (fines) and G8 (profiles 2 and 3, Fig. 5). This suggests that the contrast of the acoustic impedance among gravels (G7/G8) with sandy matrix can occur with the change in the clast-supporting style. The position of the refraction line also indicates that the contrast of the acoustic impedance between facies with sandy matrix is higher than at the boundary between the gravels with distinct content with clay and underlying gravels with sandy matrix (higher in the wells). It can be caused by continuous decrease in fines. Similarly, the contact between clays and the underlying gravels with a distinct content of clay does not produce refraction of the seismic signal. It relates probably to the matrix of the gravels, in which the clayey content is high enough to lower the contrast between the two facies. The occurrence of the line between matrix-supported gravels G5 and G7 can be caused by difference in matrix composition (content of fines), different grain size of sediments or may indicate locally clustered coarser-grained clasts within G7 causing refraction of waves. Refraction occurs also between F1 and G8 thus referring about high contrast of acoustic impedance between them.

The analysed tomographic models indicate a good correlation with the lithology of the wells. Therefore, their superimposition with wells enabled the identification of three velocity "packages" (Figs. 4, 5). The first package represents fines with velocities reaching up to 600 m/s. The second package with velocities ranging between 600 and 850 m/s was ascribed to the matrix-supported gravels with distinct content of fines, which contain mainly metamorphic and magmatic clasts (G1, G2, G4, G6 and G9). The boundary of the second package with the third one passes usually between facies G2 (above) and facies G5/G7 (below) (Figs. 4, 5). Crossing the line, few differences between the facies are recognized. At the contact of facies G2 and G7 (W2), the clay content in the matrix decreases. In other two wells (3 and 5), where the border lies between facies G2 and G5 instead of the change in matrix composition, an increase in the grain size between medium- and coarse-grained sediment is visible. Finally, the border between the packages represents change in the composition of the clasts with more metamorphic and magmatic clasts above and more carbonate clasts below.

The last package with velocities higher than 850 m/s may belong to matrix- and clast-supported gravels with a dominance of carbonates. This package contains gravels with clayey (G5) as well as sandy matrix (G7, G8), but the facies are typical by high content of carbonate clasts. The contact of the Quaternary sediments with the Neogene clays was because of its deeper position that was not identified in these models.

After 3D organization of the profiles in longitudinal and perpendicular direction (Fig. 6b), we have noticed that the second and the third packages (containing gravels) form stripes with highly variable shapes. The both stripes are typical by bended or distorted tops finally covered by overlying first unit (clays) flattening the relief. The top of the second package copies the top of the underlying third unit (matrix- to clast-supported gravels). The thickness of the stripes is stable without lateral changes. Therefore, we assume the location of the studied sediments close to the centre of the depositional systems.

Conclusions

Auger drilling is an investigation method that disturbs features of the sediments and hence limits the effectiveness of this method of drilling in developing a sound conceptual geological model of unconsolidated sediments. To summarize sedimentological and geophysical results obtained in this study, a conceptual sedimentary model of the geological system is suggested in Fig. 6.

A sedimentological approach revealed the alternating activity of stream flows and debris/hyperconcentrated flows depositing sediments as a part of fluvial and alluvial fan systems (Fig. 6a). The sediments were transported either from nearby Gemericum Unit (alluvial fan, fluvial system),

or their provenience is connected also with more distant units as the Veporicum Unit or the area of the Central-Carpathian Palaeogene Basin (fluvial system).

A seismic refraction boundary marks change between sediment support styles (clast- versus matrix-supported gravels) thus indicating also a change in depositional process between stream flows (bed load) and stream flows (bar)/hyperconcentrated/cohesionless debris flows (Fig. 4). However, refraction line can mark changes in depositional processes also between facies having the same supporting style. Here, the refraction is caused by difference in the matrix composition and grain size of sediments and delineates changes from stream flows (bar)/hyperconcentrated/cohesionless debris flows to cohesive debris flows (Fig. 5). Contact between fines and conglomerates produced refraction recording stream flows (bed load) replaced by deposition from suspension fall-out (Fig. 5).

Due to a good correlation of modelled tomographic profiles with overlapping wells, it was possible to recognize three individual velocity packages each consisting of different facies. Thus, tomographic profiles supplement the drilling data from wells and highlight the spatial distribution of facies groups. Also, they indicate the central position of studied sediments within the depositional systems (Fig. 6b). The packages vary in terms of their clay content (decreasing vertically downward) and with the composition of the clasts (dominance of metamorphic and magmatic clasts in the second package; dominance of carbonates in the third package). Combining these results with facies analysis, we can notice that each package records individual depositional system: The first package comprises an alluvial fan setting with deposition from suspension fall-out and sheetfloods; the second package comprises an alluvial fan setting with activity of hyperconcentrated/debris flows; and third package comprises a fluvial system dominated by stream flows occasionally interrupted by hyperconcentrated/debris flows (Fig. 6a). Thus, seismic tomography displays the geometry of the depositional systems in area of concern. Besides, the tomography was able to outline also the internal structure of the packages. Based on velocities inversions it was possible to recognize 1.5 m thick and 5 m long lenses (Fig. 5) as well as irregularity in Fig. 4.

In summary, the advantages of approaches used are:

- sedimentological analysis helps to identify the depositional processes and systems and provides information regarding the provenience of the sediments (Fig. 6a),
- the position of the refraction boundary refers to the main changes in the sediment texture and composition and therefore records changes between different depositional processes (Figs. 4, 5),
- seismic tomography highlights the spatial distribution and geometry of the sediments/systems, indicating the position of the sediments (facies) within the depositional systems (Fig. 6b).

Combining the knowledge regarding the origin of sediments with their geometry allows us to propose a more detailed and accurate geological model of the area.

Acknowledgements This publication is the result of the Project implementation: Research centre for efficient integration of the renewable energy sources, ITMS: 26220220064 supported by the Research and Development Operational Programme funded by the ERDF (European Regional Development Fund). We are grateful for the constructive comments of the reviewers.

References

Allen JRL (1965) A review of the origin and characteristics of recent alluvial sediments. Sedimentology 5:89–191

Amireh B (2015) Grain size analysis of the Lower Cambrian–Lower Cretaceous clastic sequence of Jordan: sedimentological and paleo-hydrodynamical implications. J Asian Earth Sci 97:67–88

Benvenuti M, Martini IP (2002) Analysis of terrestrial hyperconcentrated flows and their deposits. In: Flood and megaflood processes and deposits: recent and ancient examples. Spec. Publ. Int. Assoc. Sed., vol 32, pp 167–93

Blair TC, McPherson JG (2009) Processes and forms of alluvial fans. In: Parsons AJ, Abrahams AD (eds) Geomorphology of desert environments, 2nd edn. Springer, Berlin, pp 412–467. doi:10.1007/978-1-4020-5719-9J4

Boggs S Jr (2009) Petrology of sedimentary rocks, 2nd edn. Cambridge University Press, New York

Cheetham MD, Keene AF, Bush RT, Sullivan LA, Erskine WD (2008) A comparison of grain-size analysis methods for sand-dominated fluvial sediments. Sedimentology 55:1905–1913

DeCelles PG, Gray MB, Ridgway KD, Cole RB, Pivnik DA, Pequera N, Srivastava P (1991) Controls on synorogenic alluvial-fan architecture, Beartooth Conlomerate (Paleocene), Wyoming and Montana. Sedimentology 38:567–590

Folk RL, Ward WC (1957) Brazos River bar: a study in the significance of grain size parameters. J Sedimentar Petrol 27:3–26

Harvey AM, Mather AE, Stokes M (2005) Alluvial fans: geomorphology, sedimentology, dynamics—introduction. A review of alluvial-fan research. In: Harvey AM, Mather AE, Stokes M (eds) Alluvial fans: geomorphology, sedimentology, dynamics. Geological Society, London, Special Publications, vol 251, pp 1–7

Heward AP (1978) Alluvial fan and lacustrine sediments from the Stephanian A and B (La Magdalena, Cinera-Matallana and Sabero) coalfields, northern Spain. Sedimentology 25(4):451–488

Johnson AM (1970) Physical processes in geology. Freeman Cooper, San Francisco

Johnson AM (1984) Debris flow. In: Brunsden D, Prior DB (eds) Slope instability. Wiley, Chichester, pp 257–361

Kaličiak M, Baňacký V, Jacko S, Janočko J, Karoli S, Molnár J, Petro Ľ, Priechodská Z, Syčev V, Škvarka L, Vozár J, Zlinská A, Žec B (1991) Vysvetlivky ku geologickej mape severnej časti Slanských vrchov a Košickej kotliny, 1: 50 000. Bratislava, GÚDŠ, 231, ISBN:80-85314-11-8

Kaličiak M, Baňacký V, Janočko J, Karoli S, Petro Ľ, Spišák Z, Vozár J, Žec B (1996a) Geologická mapa Slanských vrchov a Košickej

kotliny-južná časť', M 1:50 000, Regionálne geologické mapy, Vydavateľstvo Dionýza Štúra, Bratislava, Ministerstvo životného prostredia Slovenskej republiky, Geologická služba SR, ISBN:80-85314-63-0

Kaličiak M, Baňacký V, Dubéciová S, Jacko S, Janočko J, Jetel J, Karoli S, Petro Ľ, Spišák Z, Syčev V, Zlinská A, Žec B (1996b) Vysvetlivky ku Geologickej mape Slanských vrchov a Košickej kotliny-južná časť', M 1:50 000, Vydavateľstvo Dionýza Štúra, Bratislava, ISBN:80-85314-58-4

Kim SB, Chough SK, Chun SS (1995) Bouldery deposits in the lowermost part of the Cretaceous Kyokpori Formation, SW Korea: Cohesionless debris flows and debris falls on a steep-gradient delta slope. Sed Geol 98:97–119

Komatsubara J (2004) Fluvial architecture and sequence stratigraphy of the Eocene to Oligocene Iwaki Formation, northeast Japan: channel fills related to the sea-level change. Sediment Geol 168:109–123

Kováč M, Nagymaros A, Oszczypko N, Ślączka A, Csontos L, Marunteanu M, Matenco L, Márton M (1998) Palinspastic reconstruction of the Carpathian-Pannonian region during the Miocene. In: Rakús M (ed) Geodynamic development of the Western Carpathians. Geol. Surv. Slovak Rep, Bratislava, pp 189–217

Kumar R, Suresh N, Sangode SJ, Kumaravel V (2007) Evolution of the Quaternary alluvial fan system in the Himalayan foreland basin: implications for tectonic and climate decoupling. Quat Int 159:6–20

Lavigne F, Thouret JC (2002) Sediment transportation and deposition by rain-triggered lahars at Merapi Volcano, Central Java, Indonesia. Geomorphology 49:45–69

Lowe DR (1982) Sediment gravity flows, II. Depositional models with special reference to the deposits of high-density turbidity currents. J Sed Petrol 52:279–297

Lexa J, Bezák V, Elečko M, Mello J, Polák M, Potfaj M, Vozár J (2000) Geological map of the Western Carpathians and adjacent areas 1: 500 000. Ministry of the Environment of Slovak Republic. Geological Survey of Slovac Republic, Bratislava

Major JJ (1997) Depositional processes in large-scale debris-flow experiments. J Geol 105:345–366

Nemec W (2009) What is a hyperconcentrated flow? Lecture abstract, annual meeting of th IAS, Alghero (Spain), 20–23 Sept 2009

Nemec W, Steel RJ (1984) Alluvial and coastal conglomerates: their significant features and some comments on gravelly-mass flow deposits. Sedimentology of gravels and conglomerates. In: Koester EH, Steel RJ (eds) Can. Soc. Petrol. Geol., Mem. 10, pp 1–31

Pierson TC (1970) Hyperconcentrated flow-transitional process between water flow and debris flow. In: Jakob M, Hunger O (eds) Debris-flow hazards and related phenomena, Praxis. Springer, Berlin, pp 159–202

Pierson TC, Costa JE (1987) A rheologic classification of subaerial sediment-water flows. Geol Soc Am Rev Eng Geol 7:1–12

Polák M, Jacko S, Vozárová A, Vozár J, Gross P, Harčár J, Sasvári T, Zacharov M, Baláž B, Kaličiak M, Karoli S, Nagy A, Buček S, Maglay J, Spišák Z, Žec B, Filo I, Janočko J (1996) Geologická mapa Braniska a Čiernej Hory 1:50 000. Vydavateľstvo Dionýza Štúra, Bratislava

Polák M, Jacko S, Vozárová A, Vozár J, Gross P, Harčár J, Zacharov M, Baláž B, Liščák P, Malík P, Zakovič M, Karoli S, Kaličiak M (1997) Vysvetlivky ku geologickej mape Braniska a Čiernej Hory 1:50 000. Vydavateľstvo Dionýza Štúra, Bratislava

Powers MC (1953) A new roundness scale for sedimentary particles. J Sediment Petrol 23:117–119

Remaitre A, Malet JP, Maquaire O (2005) Morphology and sedimentology of a complex debris flow in clay-shale basin. Earth Surf Process Landf 30:339–348

Serra O (1985) Sedimentary environments from wireline logs. Schlumberger, Houston

Skaberne D (1996) Interpretation of depositional environment based on grain size distribution of sandstones of the Val Gardena Formation in the area between Cerkno and Smrečje, Slovenia. Geologija 39:193–214

Sohn YK (1997) On traction-carpet sedimentation. J Sediment Res 67:502–509

Sohn YK, Rhee C, Kim BCh (1999) Debris flow and hyperconcentrated flood-flow deposits in an alluvial fan, northwestern part of the cretaceous Yongdong Basin, Central Korea. J Geol 109:111–132

Torres-Rondon L, Carriere SD, Chalikakis K, Valles V (2013) An integrative geological and geophysical approach to characterize a superficial deltaic aquifer in the Camargue plain, France. C R Geosci 345:241–250

Tucker EM (2003) Sedimentary rocks in the field, 3rd edn. Wiley, Chichester

Wagreich M, Strauss PE (2005) Source area and tectonic control on alluvial-fan development in the Miocene Fohnsdorf intramontane basin, Austria. In: Harvey AM, Mather AE, Stokes M (eds) Alluvial fans: geomorphology, sedimentology, dynamics. Geological Society, London, Special Publications, vol 251, pp 207–216

Wentworth CK (1922) A scale of grade and class terms for clastic sediments. J Geol 30:377–392

Yagishita K (1997) Paleocurrent and fabric analyses of fluvial conglomerates of the Paleogene Noda Group, northeast Japan. Sediment Geol 109:53–71

Terms and Conditions

Springer Nature journal content, brought to you courtesy of Springer Nature Customer Service Center GmbH (“Springer Nature”).
Springer Nature supports a reasonable amount of sharing of research papers by authors, subscribers and authorised users (“Users”), for small-scale personal, non-commercial use provided that all copyright, trade and service marks and other proprietary notices are maintained. By accessing, sharing, receiving or otherwise using the Springer Nature journal content you agree to these terms of use (“Terms”). For these purposes, Springer Nature considers academic use (by researchers and students) to be non-commercial.
These Terms are supplementary and will apply in addition to any applicable website terms and conditions, a relevant site licence or a personal subscription. These Terms will prevail over any conflict or ambiguity with regards to the relevant terms, a site licence or a personal subscription (to the extent of the conflict or ambiguity only). For Creative Commons-licensed articles, the terms of the Creative Commons license used will apply.
We collect and use personal data to provide access to the Springer Nature journal content. We may also use these personal data internally within ResearchGate and Springer Nature and as agreed share it, in an anonymised way, for purposes of tracking, analysis and reporting. We will not otherwise disclose your personal data outside the ResearchGate or the Springer Nature group of companies unless we have your permission as detailed in the Privacy Policy.
While Users may use the Springer Nature journal content for small scale, personal non-commercial use, it is important to note that Users may not:

1. use such content for the purpose of providing other users with access on a regular or large scale basis or as a means to circumvent access control;
2. use such content where to do so would be considered a criminal or statutory offence in any jurisdiction, or gives rise to civil liability, or is otherwise unlawful;
3. falsely or misleadingly imply or suggest endorsement, approval , sponsorship, or association unless explicitly agreed to by Springer Nature in writing;
4. use bots or other automated methods to access the content or redirect messages
5. override any security feature or exclusionary protocol; or
6. share the content in order to create substitute for Springer Nature products or services or a systematic database of Springer Nature journal content.

In line with the restriction against commercial use, Springer Nature does not permit the creation of a product or service that creates revenue, royalties, rent or income from our content or its inclusion as part of a paid for service or for other commercial gain. Springer Nature journal content cannot be used for inter-library loans and librarians may not upload Springer Nature journal content on a large scale into their, or any other, institutional repository.
These terms of use are reviewed regularly and may be amended at any time. Springer Nature is not obligated to publish any information or content on this website and may remove it or features or functionality at our sole discretion, at any time with or without notice. Springer Nature may revoke this licence to you at any time and remove access to any copies of the Springer Nature journal content which have been saved.
To the fullest extent permitted by law, Springer Nature makes no warranties, representations or guarantees to Users, either express or implied with respect to the Springer nature journal content and all parties disclaim and waive any implied warranties or warranties imposed by law, including merchantability or fitness for any particular purpose.
Please note that these rights do not automatically extend to content, data or other material published by Springer Nature that may be licensed from third parties.
If you would like to use or distribute our Springer Nature journal content to a wider audience or on a regular basis or in any other manner not expressly permitted by these Terms, please contact Springer Nature at

onlineservice@springernature.com